Journal of Achievements in Materials and Manufacturing Engineering
VOLUME 54
ISSUE 2
October
2012

Sustainability issues of research and development of forging

Y.T. Im*, S.K. Hwang, D.K. Kim, H.M. Baek, W.Y. Park, J.W. Lee, H.S. Joo, J.M. Kim
Computer Aided Materials Processing Laboratory,
Department of Mechanical Engineering, KAIST, Daejeon, Korea
* Corresponding e-mail address: ytim@kaist.ac.kr

Received 12.08.2012; published in revised form 01.10.2012

Manufacturing and processing

ABSTRACT

Purpose: of this paper is to review recent research activities of the Computer Aided Materials Processing Laboratory to improve sustainability of the material and manufacturing process in forging.
Design/methodology/approach: Empirically obtained non-dimensional equation to determine friction factor was introduced by employing tip test results. Equal channel angular processing (ECAP) and hybrid process consisting of pinch rolling, ECAP, and drawing were newly designed to make the process continuous and improve the strength of the material. The numerical program based on cellular automata and crystal plasticity was developed to predict microstructure and texture evolution during recrystallization.
Findings: The friction factors at the punch or die interfaces during cold forging can be determined separately as a function of the hardness and surface roughness of the material and punch or dies, initial yield strength of the material, viscosity of the lubricant, and die velocity. Severe plastic deformation was applied in a continuous manner and strength increase of the material was obtained as a result. The microstructure and texture evolution during recrystallization can be predicted numerically by the developed program.
Research limitations/implications: The proposed results should be compared with the practical results to further the applicability and solution accuracy.
Practical implications: The present approach can be used as an example to tackle the sustainability of the material and manufacturing process.
Originality/value: The current approach is practically easy to apply and the simulation tool developed can replace the laborious and expensive experiments.
Keywords: Tip test; Crystal plasticity finite element simulation; Cellular automata; Equal channel angular processing; Hybrid process

Reference to this paper should be given in the following way:
Y.T. Im, S.K. Hwang, D.K. Kim, H.M. Baek, W.Y. Park, J.W. Lee, H.S. Joo, J.M. Kim, Sustainability issues of research and development of forging, Journal of Achievements in Materials and Manufacturing Engineering 54/2 (2012) 147-158.

1. Introduction

Due to limitation of natural resources, producing high strength and lightweight parts with environmentally friendly process is a great challenge in the materials and manufacturing industries. The major research work related is to develop the material with better mechanical properties without adding expensive alloying elements or applying secondary processes like heat treatment and to introduce a new manufacturing process guaranteeing better quality of the products employing with the conventional material.

In practice, manufacturing engineers are faced with the problem of determining proper design of dies and tools to transform a simple billet into more complex product geometries without causing any defects at a lower manufacturing cost, depending on the material, part geometry, and process. In order to achieve this goal, mechanical parts should be produced to net-shape or near net-shape with improved mechanical properties, smooth surface finish, good dimensional accuracy, material saving, and environmental friendliness, depending on service requirements. Thus, near net-shape manufacturing has been evolved into a "must" condition for industry in meeting new demand for reducing manufacturing cost together with better sustainability.

Since the decision made at the process design level has profound effect on the dies and tools design, manufacturing, maintenance, and life cycle of the tools, a great deal of investigations have been made to reduce an experience-based process development in industry. After the pioneering work by Lee and Kobayashi [1], the application of computers in manufacturing has been growing rapidly and independently in the area of computer aided design, computer aided manufacturing, computer aided process planning and rapid prototyping to aid design and manufacturing activities at practice.

Some applications of such activities, computer-aided design systems for three-dimensional extrusion process to manufacture gears, roll pass and profile design in bar rolling, and flat-die hot extrusion process were developed with the help of finite element analyses [2-11]. In order to investigate tool life of forming dies, elastic analyses were made in couple with the rigid thermo-viscoplastic approach to simulate the deformation [12-18]. The microstructure evolution during hot deformation and heat treatment were also analyzed in order to control mechanical property during the process [19-29]. In addition, a novel technique was introduced to characterize the friction conditions in cold forging by tip test considering the deformation speed, surface roughness, and various lubricants [30-38].

In the present paper, recent development made at the computer aided materials processing laboratory will be introduced in the areas of empirical determination of the dimensionless equation for the shear friction factor in cold forging by the tip test [39]; development of process sequence design for manufacturing a high-strength bolt of fully pearlitic high-carbon steel [40,41]; continuous high-strength aluminum bolt manufacturing process design by the spring-loaded equal channel angular processing (ECAP) system [42-49], development of a continuous hybrid process for manufacturing high-strength carbon steel [50-53], crystal plasticity finite element simulation of anisotropic behavior of fine-grained material processed by the ECAP [54,55], and cellular automata simulation of microstructure and texture evolution during recrystallization in the hot deformation [56-58].

2. Determination of empirical equation for the shear friction factor in cold forging

Friction is a highly non-linear phenomenon affected by a number of process parameters such as material property, characteristics of lubricant, deformation speed, temperature, surface condition, tool geometry, environmental factors, and their interactions.

Although there have been a number of friction tests, it is still unclear whether these techniques are useful enough to differentiate the effect of these parameters on friction separately. In this regard, Im and co-workers [30,31] introduced a novel test method called tip test based on a combination of simple compression and backward extrusion at room temperature in which a radial tip was formed on the extruded end of the specimen to evaluate the friction and lubrication more accurately, as shown in Figure 1. With this test, the friction conditions at the punch, side wall, and counter punch were characterized accurately and separately [32-39].

In Figure 2, the plots of determined shear friction factors at the punch interface m_{fp} versus deformation speed are provided as an example. In this figure, the shear friction factors at the punch interface increased exponentially for the case of grease as deformation speed increased. However, they decreased exponentially for the cases of liquid lubricants. According to this result, decrease in the shear friction factor at the punch interface

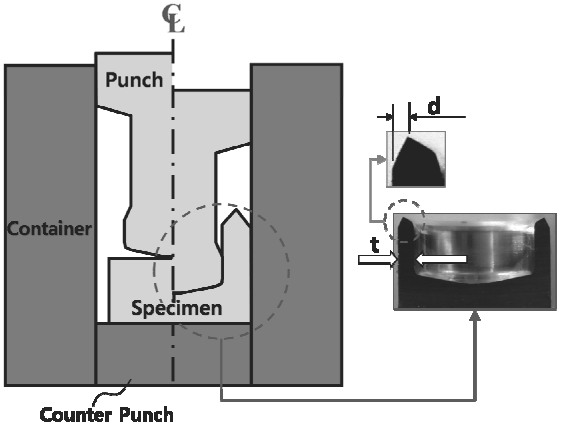

Fig. 1. Schematic of the tip test [30]

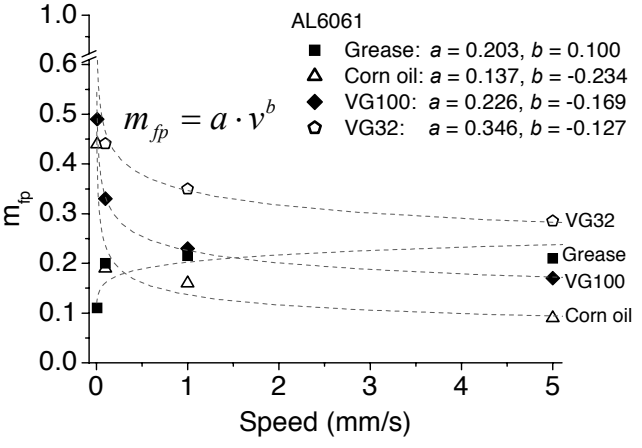

Fig. 2. Comparison of shear friction factors at the punch interface (m_{fp}) versus deformation speed (v) with different lubricants [35]

can be interpreted as reduction in the solid-solid contact area and contact pressure at the asperities due to counterbalancing hydrodynamic pressure of the liquid lubricants [37].

Based on such studies, Jung et al. [39] empirically derived the following dimensionless equation to determine the shear friction factor at the counter punch interface,

$$m_{fd} = 0.03 \log\left\{\left(\frac{H_{counter}}{H_{mat}}\right)^{7.3} \cdot \left(\frac{R_{a\,counter}}{R_{a\,combined}}\right)^{4.0} \cdot \left(10^{-9}\frac{r \cdot \sigma_y}{v \cdot \eta}\right)^{\gamma}\right\} = 0.03\Omega$$

$$\gamma = \begin{cases} 4.0 & \text{for the VG series} \\ 3.3 & \text{for corn oil} \\ 0.2 & \text{for grease} \end{cases}$$

where $0 \le m_{fd} \le 1$.

By looking into this dimensionless equation, the effect of physical and process variables on the friction investigated can be estimated without carrying out any further experiments. This enables us to easily control and predict the friction a priori depending on the given processing conditions. According to this equation, selection of the die material ($H_{counter}$, hardness) compared to the deforming material (H_{mat}, hardness) is mostly important to determine the friction level in cold forging as expected. The secondly important term is the ratio between the surface roughness of the counter punch ($Ra_{counter}$) and the combined value ($Ra_{combined}$, refer to reference [39]) according to this equation. The thirdly important term represents the effect of processing variables represented by actual dimension (r, radius of the billet) and yield strength of the specimen (σ_y), deformation speed (v), and the viscosity of the lubricant (η) on the friction and is relatively less important according to this equation.

Since numerical prediction of the friction level can be made as a function of Ω by utilizing this equation as shown in Figure 3, it is easy to apply this equation for determining the shear friction factors for the punch and counter punch for numerical and theoretical applications, and the scientific selection of the processing variables can be feasible for industrial applications as well.

3. High-strength bolt manufacturing by new approaches

In the following section, two approaches to manufacture the high strength products will be demonstrated by using the bolt forming as an example for convenience; one by introducing fine-grained initial specimens prepared by the ECAP and the second by employing a new manufacturing process sequence design employing with the conventional material.

ECAP is an effective method that induces severe plastic deformation through the channel with an equal cross-section. In Figure 4, the ECAP designed by Jin et al. [42,43] is shown to produce the fine-grained aluminum alloy of AA1050. During the ECAP, route A refers to pressing the billet repetitively without any rotation, route Bc refers to a rotation of 90° in a counterclockwise direction between each pass, and route C refers to rotating 180° between each pass. In Figure 5, multi-stage forming sequence is introduced to form high strength aluminum bolts sequentially at room temperature.

According to their work, conventional bolt forming consisted of two stages of preforming and final heading. On the other hand, the fine-grained specimen required an extra preforming stage of tapered extrusion due to change of formability of the specimen as shown in Figure 6 as reported by Choi et al. [44].

In the ECAP, three passes with three different routes were applied in order to investigate the effect of processing routes and the number of passes on strength increase as shown in Figure 7. For route A, the ultimate tensile strength (UTS) increased from 128 to 182 MPa after a single pass and up to 198 MPa after three passes. For routes Bc and C after three passes, UTS also increased to 205 and 196 MPa, respectively. On the other hand, elongation of the fine-grained specimen relatively decreased by 15.5% compared to the conventional one. The reason for the increased strength was mostly owing to grain refinement through the ECAP.

According to transmission electron microscopy reported by Jin et al. [45] as shown in Figure 8, the grain size became smaller and elongated to about 1 μm after one pass of the ECAP from 100 μm in the original specimen. However, the grain size did not decrease significantly with increasing number of passes. Similarly, increase in strength was negligible after two or three passes in the tension test. Thus, single pass ECAP might be enough to obtain higher strength for bolt manufacturing in terms of lesser manufacturing cost required.

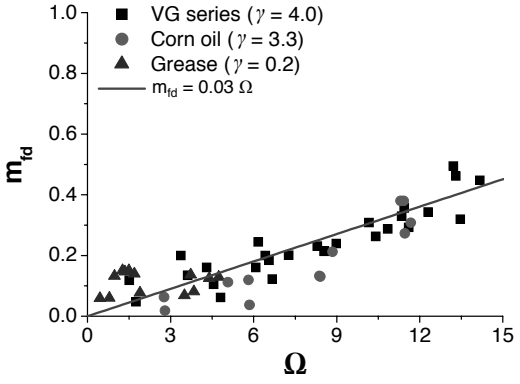

Fig. 3. Dimensionless equation for the shear friction factor determined [39]

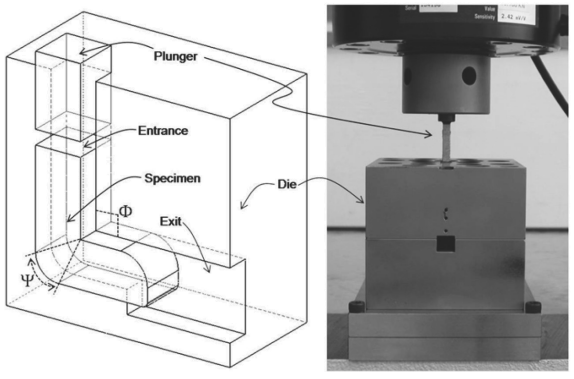

Fig. 4. schematic illustrations of the die geometry and experimental set-up for the ECAP process [42,43]

Fig. 5. The aluminum bolt manufactured by the ultra-fine grained specimen [44]

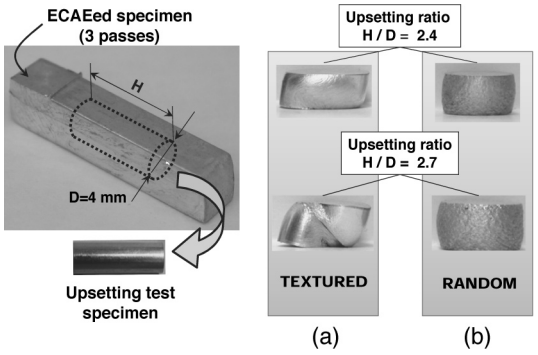

Fig. 6. Example of deformation anisotropy induced by texture in the work by Choi et al. [45]: deformed shapes after upsetting of (a) the three-pass ECAPed specimen processed by route C (textured) and (b) the fully annealed specimen (random)

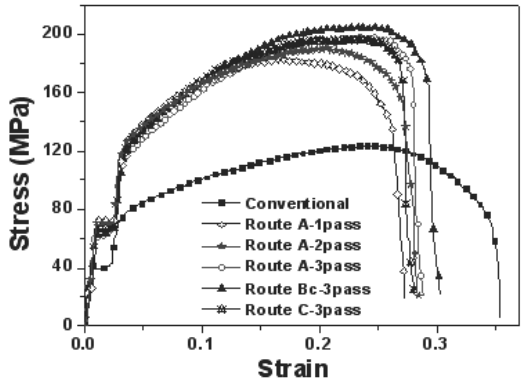

Fig. 7. Increase of the UTS with three different routes [44]

In Figure 9, fully pearlite high-carbon steel, known as a higher delayed fracture strength material, with an ultimate tensile strength of 1410 Mpa was used for manufacturing a high-strength M8 bolt by Lee et al. [46,47]. The original material shows a softening behavior. Based on the preform made by extrusion, the bolt was successfully manufactured with the strength of 1600 Mpa.

The delayed fracture strength was also improved with the developed bolt compared to the data of a conventional high-strength bolt as shown in Figure 10.

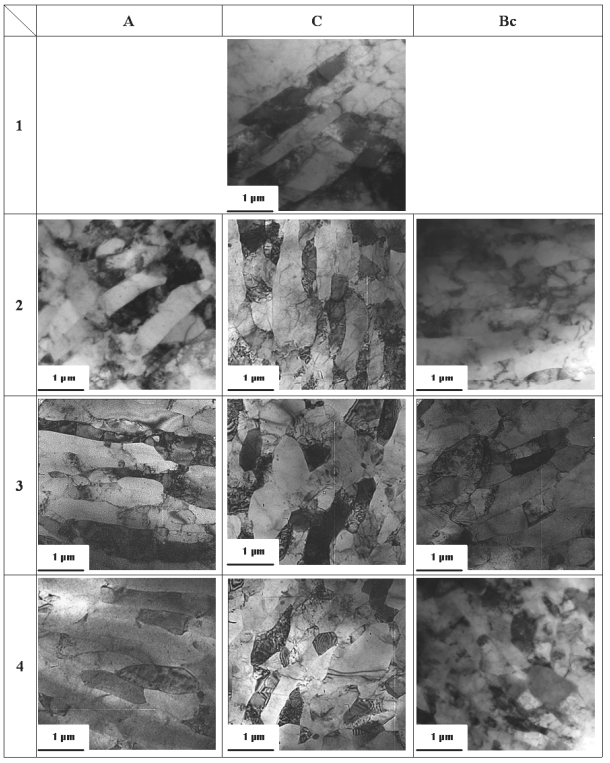

Fig. 8. Microstructure changes of the processed specimens in the cross-section parallel to the extrusion direction for routes A, C and Bc up to four passes [45]

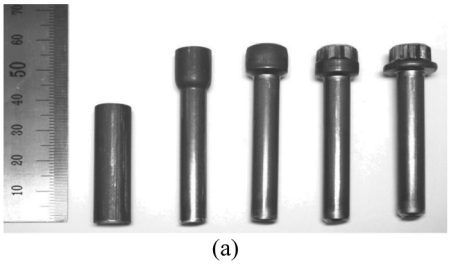

(a)

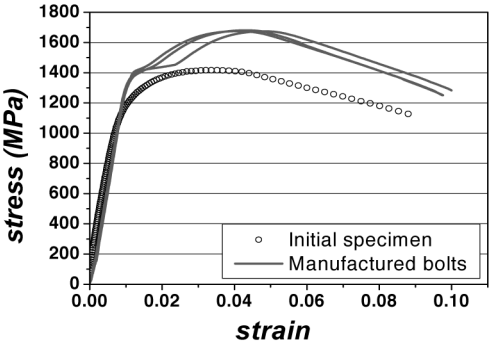

(b)

Fig. 9. (a) The high strength bolt manufactured by the pearlite specimen and (b) tensile test results of the initial specimen and manufactured bolts [46]

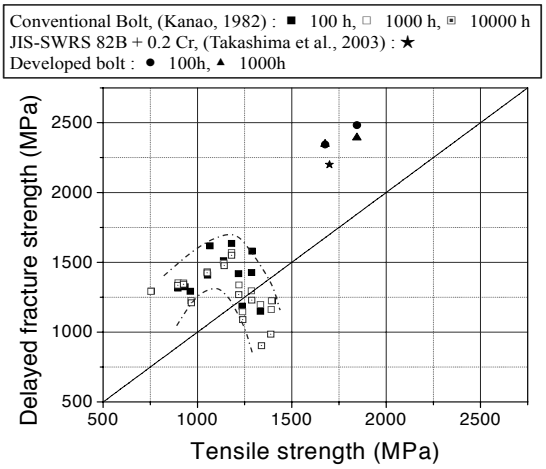

Fig. 10. Comparison of delayed fracture strength for the developed and conventional bolts [46]

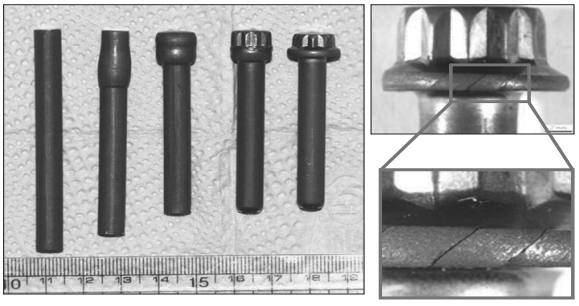

Fig. 11. Manufactured bolt and preforms formed by the upsetting-based process design [46]

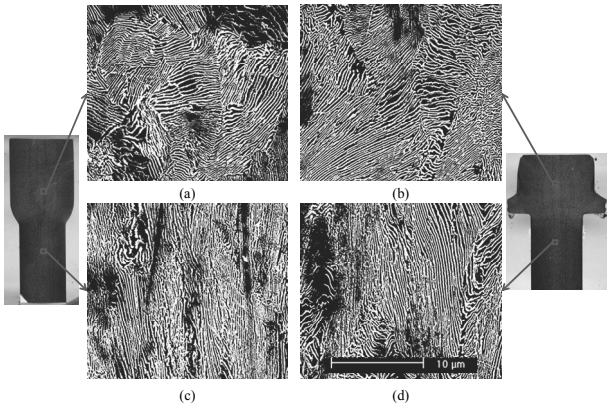

Fig. 12. Changes of microstructures at two different locations of the developed bolt and its preform by SEM [46,47]

If the upsetting-based preform was used for the second preform then, the cracking occurred at the flange of the bolt head owing to the frictional effect as shown in Figure 11. This fracture can be removed by using the better lubricated specimen in the work by Jin et al. [48].

Figure 12 shows microstructures at the head and body part of the developed bolt and its preform observed by scanning electron microscope (SEM). During the extrusion process, the lamellar structure of pearlite was rearranged to the direction of extrusion and the inter-lamellar spacing became narrower as shown in Figure 12(c), compared to the non-extruded part in Fig. 12(a). Since no further deformation was applied to the body part after extrusion, microstructure of the body in Fig. 12(d) was very similar to that of the extruded part at the first stage. Because of the microstructural changes, the mechanical behaviors were improved in the bolt manufactured by the fully pearlite material with the new process sequence introduced here.

4. Development of a continuous hybrid process

It is well known that above-mentioned ECAP is limited on a laboratory scale and applications of the process are probably only effective in manufacturing expensive products, where the production cost is not a major concern. Therefore, Jin et al. [48,49] proposed split dies combined with a spring-loaded auto-fastening system to continuously apply the ECAP process to multi-pass bolt-forming process. They successfully manufactured the fine-grained aluminum bolts, which had higher UTS and elongation compared to the conventionally made bolts in a continuous sequence by using the spring-loaded ECAP system. Despite these efforts, the ECAP process has difficulty in producing long products. In this regard, the hybrid process, which can provide a continuous wire with better mechanical properties, could be favorable from a practical standpoint.

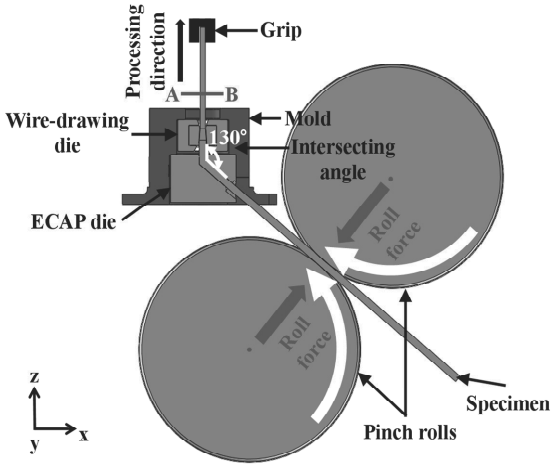

Fig. 13. Schematic diagram of the hybrid process reproduced from Hwang et al. [50]

According to the works by Hwang et al. [50,51] and Baek et al. [52], a hybrid process consisting of several dies such as pinch rolls, ECAP dies, and a wire-drawing die, as shown in Figure 13,

can produce high-strength material in a continuous manner. As shown in Figure 14, the hybrid process enabled the continuous manufacturing of the wire with grain refinement, good surface quality, and dimensional accuracy. The material flow was controlled by the pulling velocity of the grip and the angular velocity of the pinch rolls. The main driving force is tension applied by pulling the grip and the frictional force between the workpiece and pinch rolls, which pushed the specimen into the ECAP die to suppress the cross-sectional reduction by tension. The ECAP and wire-drawing dies applied shear deformation to the specimen and skin-pass sizing of the deformed specimen for dimensional accuracy, respectively.

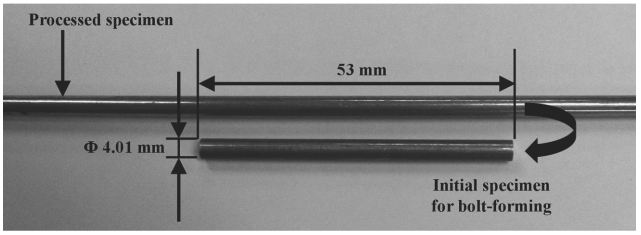

Fig. 14. Continuous grain-refined AA6061 wire processed by the two-pass hybrid process and an initial cylindrical specimen for bolt-forming cut from the wire [53]

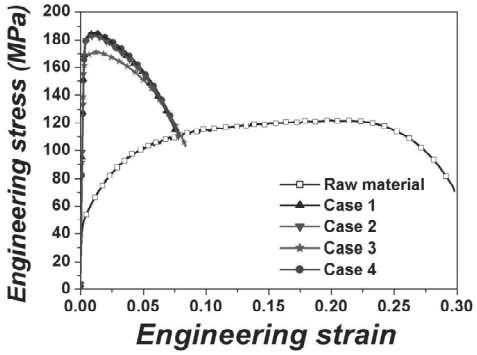

Fig. 15. Stress–strain curves obtained from the tension tests [53]

In the recent work by Kim et al. [53], fine-grained AA6061-O wire was manufactured by a two-pass hybrid process in a continuous manner to improve the mechanical strength of the material through grain refinement and to investigate the effects of processing routes for two different routes, A and C, on the improvement of mechanical properties. Finally, high-strength M4.5 bolts with a long body part and with 0.5 mm pitch according to JIS B0251 for demonstrating the practical application of the hybrid process were manufactured using the fine-grained AA6061-O wire processed by the two-pass hybrid process with routes A and C to achieve 50% higher UTS compared to the raw material, roughly 180 MPa. As a result, the practicality of the hybrid process to easily couple with conventional wire production will be demonstrated to achieve the grain refinement of the material.

For convenience, the case numbers of Case 1 (two-pass hybrid process with route A), Case 2 (two-pass hybrid process with route C), Case 3 (two-pass wire-drawing), and Case 4 (three-pass wire-drawing) were introduced to differentiate the experimental conditions in their work.

According to the tension test results in reference [53], the UTS of the original AA6061-O specimen was 122 MPa, as shown in Figure 15. For Cases 1, 2, 3, and 4, the UTS values increased to 185 MPa, 183 MPa, 171 MPa, and 184 MPa, in that order. On the other hand, elongations decreased from 29.8% to 7.5%, 7.8%, 8.4%, and 7.8%, in the same order. From the results of Cases 1 and 2, little differences in the UTS value and elongation were observed between routes A and C in the two-pass hybrid process. From the results of Cases 1 and 3, the specimen processed by the two-pass hybrid process of route A showed an 8.2% higher UTS value than in the two-pass wire-drawing case, although elongation was slightly lower than the one processed by the two-pass wire-drawing process due to the accumulation of plastic deformation. Furthermore, the specimen processed by the two-pass hybrid process showed similar UTS value and elongation with the one processed by the three-pass wire-drawing process. From these results, the hybrid process improved the mechanical properties more effectively than the conventional wire-drawing process and reduced the number of passes to obtain a similar UTS level. It was found from this work that the two-pass wire-drawing was insufficient to achieve the 180 MPa UTS requirement according to the experimental results.

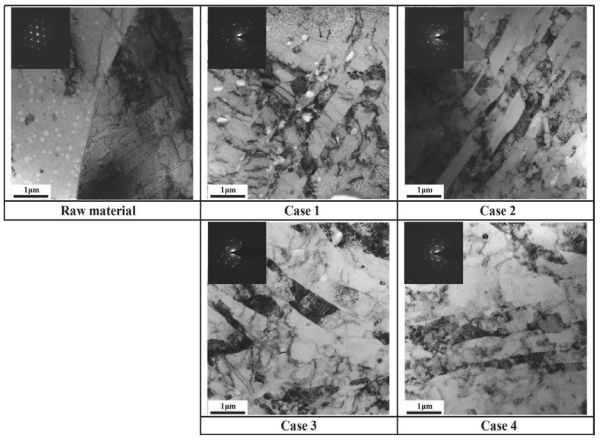

Fig. 16. TEM images obtained from the annealed AA6061-O specimen and the specimens processed by four different processing conditions [53]

It can be also seen in Figure 16 that original grains were subdivided and elongated for all cases due to the accumulation of dislocations and the formation of subgrain boundaries was observed owing to plastic deformation. In order to obtain the selected area electron diffraction (SAED) pattern, the same aperture size was used for all cases. The SAED patterns consisted of rings with many diffracted beams so that there were many small grains with multiple orientations within the selected fields of view. Therefore, the SAED pattern indicates that the specimen processed by each case had fine grains, potentially with higher angle grain boundaries, compared to the annealed initial specimen. It can be seen in this figure that grains in the specimen processed by the Case 2 (two-pass hybrid with route C) showed

smaller deformation bands and had potentially higher angle grain boundaries compared to the specimen processed by the Case 3 (two-pass wire-drawing). There is no difference between Cases 2 and 4 (three-pass wire-drawing) in this figure, similar to the UTS results. Owing to the previous study by Hwang et al. [49], the areal fraction of low angle grain boundaries was significantly increased by the one-pass hybrid process compared to the one-pass wire-drawing process. Based on these observations, the hybrid process could effectively impose large plastic deformation on the material and could more efficiently manufacture wire with grain refinement compared to the wire-drawing process at the same number of passes.

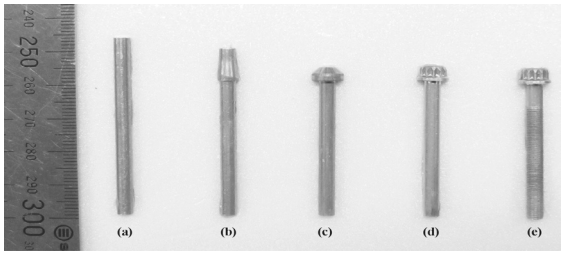

Fig. 17. Three stages of the bolt-forming process for the fine-grained specimen: (a) initial specimen, (b) first preform, (c) second preform, (d) final heading, and (e) threaded bolt by thread rolling [53]

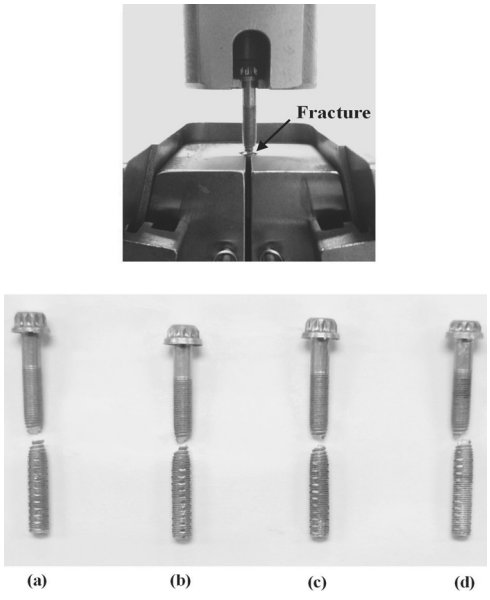

Fig. 18. Fracture behaviors of the manufactured bolts obtained from the bolt tension test for (a) Case 1, (b) Case 2, (c) Case 3, and (d) Case 4 [53]

The high-strength bolts using the fine-grained AA6061-O wire processed by the two-pass hybrid processes were successfully manufactured as shown in Figure 17. In Figure 18, a ductile fracture was observed in the bolt tension test of the manufactured bolt meeting the requirement by the ASTM standard. The fracture of the manufactured bolt for each case occurred at the first thread right above the jaw, and the ductile fracture occurred for each case as necking took place before the fracture in this figure. Therefore, the hybrid process can be applied in high-strength bolt manufacturing with no limitations on the length of the bolt.

5. Crystal plasticity FE simulations

Upsetting tests of the cylindrical specimens extracted from the ECAP were extensively examined in the work by Choi et al. [46]. The crystal plasticity finite element (CPFE) method, which incorporated the crystal plasticity constitutive law into the three-dimensional finite element (FE) method, was developed to investigate the textural evolution and deformation anisotropy during the bulk forming process of the grain-refined specimen obtained from the ECAP.

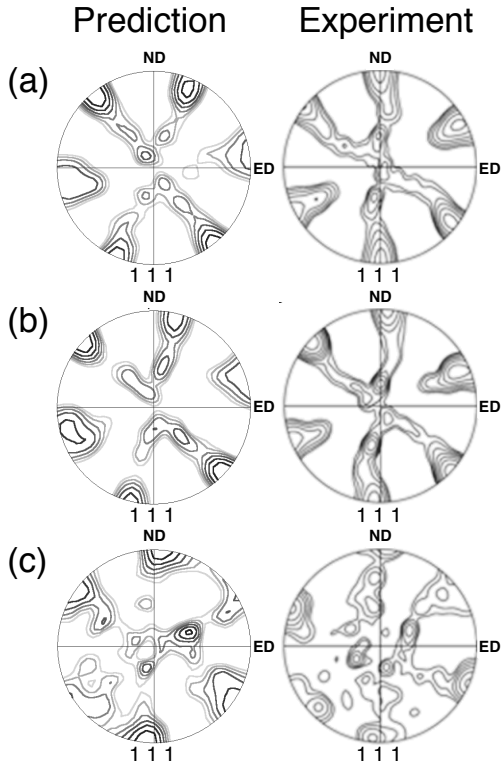

Fig. 19. Comparison of the predicted (1 1 1) pole figures with the corresponding experiments after the single pass ECAP: (a) upper deformation path, (b) middle deformation path, and (c) lower deformation path [54]

A rate-dependent polycrystalline theory was fully implemented into an in-house program, CAMP*form*3D developed by Kim and Im [12,13] and each integration point in the element

was considered to be a polycrystalline aggregate consisting of a large number of grains. In order to predict the anisotropic behavior in the subsequent upsetting test specimen efficiently, a sequential analysis techniques consisting of decoupled and coupled CPFE analyses were proposed by Jung et al. [54,55].

Firstly, the rigid-viscoplastic FE analyses of the ECAP were carried out to determine the history of velocity gradient during the process to identify the effect of the processing routes A and C of the ECAP on texture evolution. The calculated history was applied to the crystal plasticity model to obtain the crystallographic texture distribution for improving computation efficiency.

Secondly, CPFE analysis was used for prediction of the anisotropic behavior of the subsequent upsetting specimen with a full FE model. In order to reflect the texture evolution on the deformation analysis, transfer algorithms were developed for implementation of the developed algorithm. The numerical results indicated that the currently developed simulation technique with the transfer algorithms can be used effectively to simulate deformation induced anisotropy in the subsequent deformation of commercially pure aluminum AA1050 after being processed by the ECAP.

The difference of the deformation history could highly influence the textural changes in each deformation path. After one pass ECAP the predicted textures from the decoupled analysis are compared with the corresponding experimentally measured results in Figure 19(a)-(c) for the different locations across the billet thickness. The textures in Figure 19(a) and (b) are characteristic of the shear textures. It can also be seen that the texture differences between the upper and the middle of the billet after one pass are relatively minimal. However, the textures for the lower path are substantially different from those for the upper and the middle of the billet in this figure.

There are some differences between the prediction and the experimental results for the upper and the lower path due to the differences in the dimensions of the dies and workpiece between the simulation and the experiment reported in the literature. Especially, it is reported that the textures developed in the material are dependent on the die intersecting angle and corner angle.

A square specimen with a width, thickness, and length of $5.0 \times 5.0 \times 25.0$ mm^3 was subjected to the three-pass ECAP for the two processing routes A and C [46]. Route A refers to pressing the sample repetitively without any rotation, and route C refers to rotating by 180° between each pass as mentioned earlier. The predicted pole figures after each pass for the route A and C are compared in Figure 20(a)-(c) and (d)-(f), respectively.

In the case of route A, it was found that the overall texture was getting strong as the number of passes increased as inferred by the maximum values of Figure 20(a)-(c), even though the developing texture components are somewhat different for each pass. In route C, the shearing occurred on the same plane in each consecutive pass and the shear direction was reversed in the following pass. Since the middle of the billet has experienced forward and reverse shear during the two passes of route C, it may be expected that the initial texture would be recovered. However, it is reported that the textures in the even numbered passes do not recover initial texture and have retention of shear texture in the experimental findings available in the literature. In contrast, the prediction using the velocity gradient history from the FE analysis could predict the retained shear type textures even in the even numbered pass as shown in Figure 20(d)-(f). Since the FE analysis can capture the material deformation behavior such as the small tensile and compressive strains, and friction at the contact with the dies, it is not a complete reversal compared to the assumed simple shear model. Therefore, it would be essential to use the FE deformation history for capturing this subtle change in texture.

For the subsequent upsetting simulation having upsetting ratio (height/diameter) of 2.4 in route A, it was found that the deformation of the workpiece shown in Figure 21(a) was inhomogeneous unlike the deformation predicted by the conventional FE analysis as shown in Fig. 21(b). The simulated result is similar to the deformed shape obtained from the experiment as shown in Fig. 21(c). Furthermore, the material flow in the outer part of the deformed workpiece was anisotropically deformed to produce sigmoidal type pattern in Figure 22.

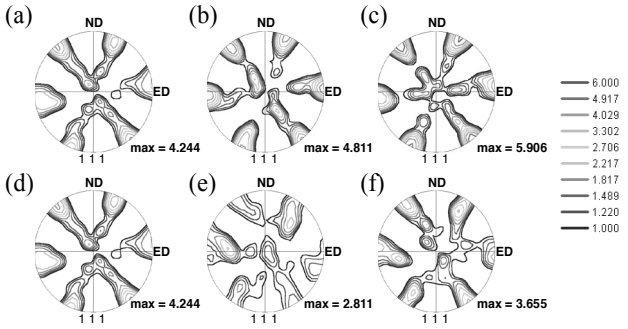

Fig. 20. Contours of (1 1 1) pole figures for (a) the first pass, (b) the second pass, and (c) the third pass in the route A, and (d) the first pass, (e) the second pass, and (f) the third pass in the route C [55]

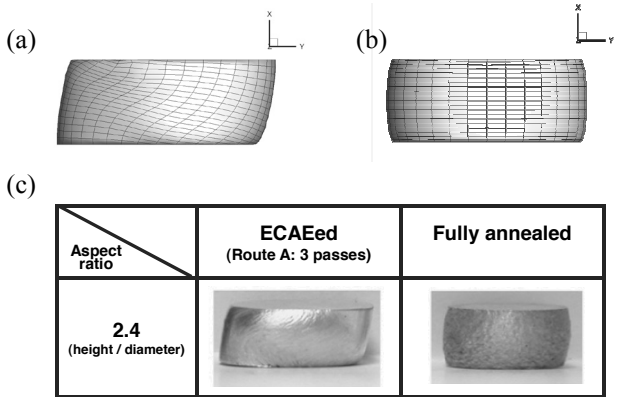

Fig. 21. Comparison of the deformed shapes predicted by using (a) the CPFEM and (b) the conventional FEM, and (c) experimental results of the upsetting tests after the three-pass ECAP (route A with aspect ratio of 2.4) and the fully annealed [55]

In order to investigate the effect of friction condition between the dies and the material on the deformed shape of the workpiece, two different friction factors of 0.04 and 0.08 were also tried according to the works by Lee et al. [42] and Son et al. [43]. As shown in Figure 23, it was found that the deformation behavior was very sensitive to the friction condition and the case of 0.04 showed the most similar result with the experiment.

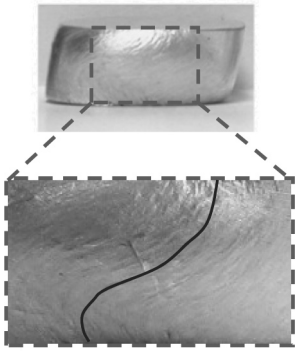

Fig. 22. material flows at the side after the upsetting of ECAPed specimen (route A with aspect ratio of 2.4) [55]

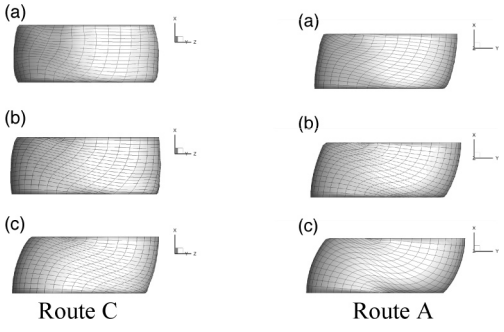

Fig. 23. Effect of the friction conditions on the deformation behavior of the subsequent upsetting of the three-pass ECAPed specimen with aspect ratio of 2.4 for route C and A, respectively: (a) m_f =0.12, (b) m_f =0.08, and (c) m_f =0.04 [55]

Since there is no symmetric plane in the simulation, there is no particular constraint against the deformation except for the velocity boundary condition in the upsetting direction (x direction) due to die contact in that direction. Therefore, friction between the dies and the material could act as a crucial constraint preventing the material from deforming freely. In addition, it was found that the case of route A showed the similar tendency for the friction factor as shown in the same figure.

6. Cellular automata simulations

In automobile industry, there is great demand to apply high-strength metals for weight reduction owing to environmental and energy concerns. Recrystallization (RX) governs the final grain size of the material. During the RX process, new grains originate and the resulting microstructure varies with the deformation condition. Therefore, understanding the RX is of importance when attempting to control the mechanical properties of a material by grain refinement.

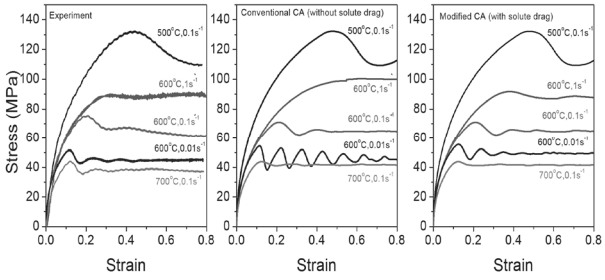

Fig. 24. Comparison of flow stress curves obtained by the isothermal hot compression tests and CA analyses [56]

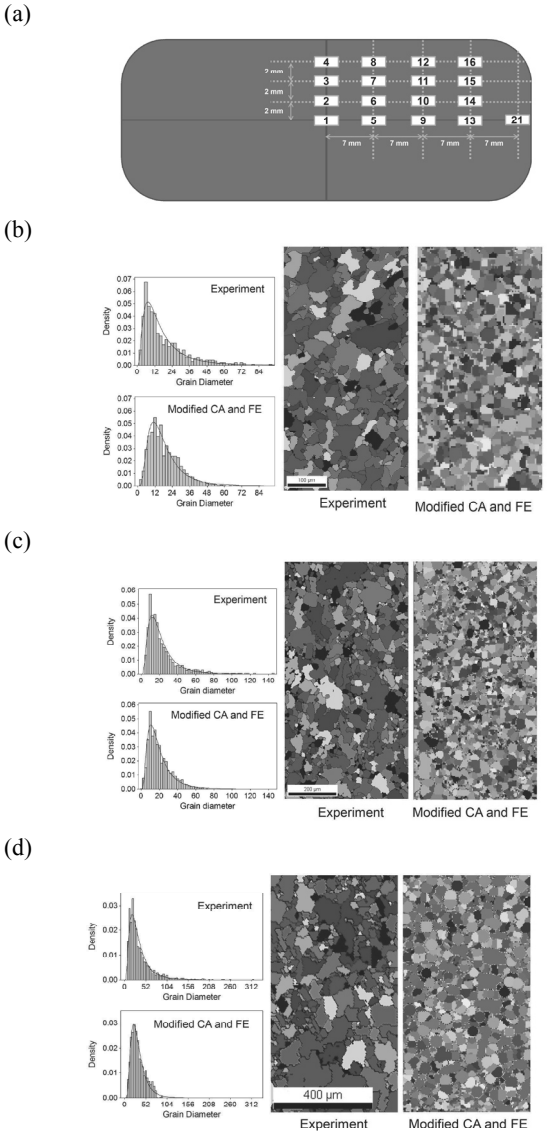

Fig. 25. (a) Configuration of measured points by EBSD of nonisothermal experiment and comparison of grain distribution and microstructure at points (b) 1, (c) 9, and (d) 12 between the nonisothermal experiment and the current numerical scheme [57]

In the work by Lee et al. [56,57], dynamic RX during non-isothermal hot compression of copper was numerically simulated by cellular automata and finite element analysis. A modified cellular automata model was developed by introducing a new parameter for considering solute drag effect. Figure 24 shows the effect of solute drag on prediction of the flow stress behaviour during non-isothermal hot compression.

The local changes of microstructure and average grain size were simulated by cellular automata and compared with the experimental results in Figure 25. The simulation results were in reasonably good agreement with experimentally measured data obtained by electron backscattering diffraction.

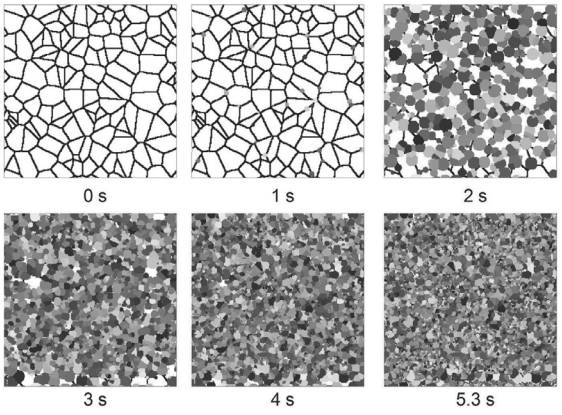

Fig. 26. Simulated microstructures at point 1 during the nonisothermal compression [57]

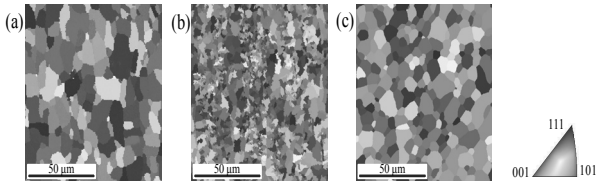

Fig. 27. The recrystallized microstructures: (a) experimental and (b) numerical without CDP and (c) with CDP, respectively [58]

Figure 26 shows changes of the simulated microstructure at point 1. The nucleation was started at about 1 s, the prior grain boundaries were mostly used as nucleation sites. Therefore, further RX occurred mostly at the recrystallized grain after 2 s. In result, the final microstructure was mostly recrystallized. The developed scheme can be applied to control grain refinement during dynamic recrystallization in the hot forging process.

This work further extended to simulate primary static RX of interstitial free (IF) steel by Kim et al. [58]. In this work, the effect of curvature-driven pressure (CDP) on the microstructural and textural evolution during RX was investigated as shown in Figure 27.

7. Conclusions

Various aspects of research topics involved with sustainable research and development of forging process are demonstrated in this review paper. Although the given examples are limited to cold forging, it is quite interesting to understand the notion of the new research directions and initiatives. According to the research works carried out so far, it is important to characterize the frictional condition properly and link the material and process aspects together to the manufacturing process design to make the process sustainable. In order to achieve these goals utilization of the proper simulation tools, development of design system, and understanding of the material behavior due to the microstructure and texture evolution depending on the process condition are necessary.

Acknowledgements

The author expresses special thank for the generous grants from the Ministry of Education, Science and Technology through National Research Foundation (No. R0A-2006-000-10240-0) and POSCO without which these works were not possible. In addition special thanks go to Drs. H.C. Lee, Y.G. Jin, K.H. Jung, and K.H. Jung, including former graduates of the Laboratory for their contributions in preparing the manuscript.

References

[1] C.H. Lee, S. Kobayashi, New Solutions to Rigid-Plastic Deformation Problems using a Matrix Method, Journal of Engineering for Industry-Transactions of the ASME 95 (1973) 865-873.
[2] H.S. Kim, Y.T. Im, Expert System for Multi-Stage Cold-Forging Process Design With a Re-Designing Algorithm, Journal of Materials Processing Technology 54 (1995) 271-285.
[3] H.S. Kim, Y.T. Im, Muti-Stage Cold Forging Process Design with A* Searching Algorithm, Trans NAMRI/SME 24 (1996) 161-166.
[4] H.S. Kim, Y.T. Im, An Expert System for Cold Forging Process Design based on a Depth-First Search, Journal of Materials Processing Technology 95 (1999) 262-274.
[5] J.H. Song, Y.T. Im, Expert System for Process Sequence Design of a Ball Stud, Journal of Materials Processing Technology 89 (1999) 72-78.
[6] J.H. Song, Y.T. Im, Development of a Computer-Aided-Design System of Cold Forward Extrusion of a Spur Gear, Journal of Materials Processing Technology 153-154 (2004) 821-828.
[7] J.H. Song, Y.T. Im, Process Design for Closed-Die Forging of Bevel Gear by Finite Element Analyses, Journal of Materials Processing Technology 192-193 (2007) 1-7.
[8] G.A. Lee, D.Y. Kwak, S.Y. Kim, Y.T. Im, Analysis and Design of Flat Die Extrusion Process 1. Three-Dimensional Finite Element Analysis, International Journal of Mechanical Sciences 44 (2002) 915-934.
[9] G.A. Lee, Y.T. Im, Analysis and Die Design of Flat Die Extrusion Process 2. Numerical Design of Bearing Lengths, International Journal of Mechanical Sciences 44 (2002) 935-946.

[10] S.H. Kim, Y.T. Im, A Knowledge-based Expert System for Roll Pass and Profile Design for Shape Rolling of Round and Square Bars, Journal of Materials Processing Technology89 (1999) 145-151.
[11] H.C. Kwon, Y.T. Im, Interactive Computer-Aided-Design System for Roll Pass and Profile Design for Shape Rolling of Round and Square Bars, Journal of Materials Processing Technology 123 (2002) 399-405.
[12] S.Y. Kim, Y.T. Im, Three-Dimensional Finite Element Simulation of Shape Rolling of Bars, Int. International Journal of Forming Processes 3 (2000) 253-278.
[13] S.Y. Kim, Y.T. Im, Three-Dimensional Finite Element Analysis of Non-Isothermal Shape Rolling, Journal of Materials Processing Technology 127 (2002) 57-63.
[14] D.Y. Kwak, J.S. Cheon, Y.T. Im, Remeshing for Metal Forming Simulations - Part I: Two-Dimensional Quadrilateral Remeshing, International Journal for Numerical Methods in Engineering 53 (2002) 2463-2500.
[15] D.Y. Kwak, Y.T. Im, Remeshing for Metal Forming Simulations - Part II: Three-Dimensional Hexahedral Mesh Generation, International Journal for Numerical Methods in Engineering 53 (2002) 2501-2528.
[16] W.Y. Choi, D.Y. Kwak, I.H. Son, Y.T. Im, Tetrahedral Mesh Generation based on Advancing Front Technique and Optimization Scheme, International Journal for Numerical Methods in Engineering 58 (2003) 1857-1872.
[17] W.Y. Choi, I.H. Son, Y.T. Im, Locally Refined Tetrahedral Mesh Generation based on Advancing Front Technique with Optimization and Smoothing Scheme, Communications in Numerical Methods in Engineering 20 (2004) 681-688.
[18] H.C. Lee, J.S. Choi, K.H. Jung, Y.T. Im, Application of Element Deletion Mthod for Numerical Analyses of Cracking, Journal of Achievements in Materials and Manufacturing Engineering 35 (2009) 154-161.
[19] H.C. Kwon, Y.S. Lee, Y.T. Im, Experimental and Numerical Prediction of Austenite Grain Size Distribution in Round-oval Shape Rolling, ISIJ International 43 (2003) 1967-1975.
[20] M.A. Saroosh, H.C. Lee, Y.T. Im, S.W. Choi, D.L. Lee, High Cycle Fatigue Life Prediction of Cold Forging Tools Based on Workpiece Material Property, Journal of Materials Processing Technology 191 (2007) 178-181.
[21] H.C. Lee, Y. Lee, S.Y. Lee, S. Choi, D.L. Lee, Y.T. Im, Tool Life Prediction for the Bolt Forming Process Based on High-Cycle Fatigue and Wear, Journal of Materials Processing Technology 201 (2008) 348-353.
[22] H.C. Lee, M.A. Saroosh, J.H. Song, Y.T. Im, The Effect of Shrink Fitting Ratios on Tool Life in Bolt Forming Processes, Journal of Materials Processing Technology 209 (2009) 3766-3775.
[23] H.C. Kwon, Y.S. Lee, S.Y. Kim, J.S. Woo, Y.T. Im, Numerical Prediction of Austenite Grain Size in Round-Oval-Round Bar Rolling, ISIJ International 43 (2003) 676-683.
[24] H.W. Lee, H.C. Kwon, Y.T. Im, P.D. Hodgson, Numerical Investigation of Austenite Grain Size Distribution in Square-Diamond Pass Hot Bar Rolling, Journal of Materials Processing Technology 191 (2007) 114-118.
[25] H.C. Kwon, H.W. Lee, H.Y. Kim, Y.T. Im, H.D. Park, D.L Lee, Surface Wrinkle Defect of Carbon Steel in the Hot Bar Rolling Process, Journal of Materials Processing Technology 209 (2009) 4476-4483.
[26] K.H. Jung, H.W. Lee, Y.T. Im, Numerical Prediction of Austenite Grain Size in a Bar Rolling Process Using an Evolution Model Based on a Hot Compression Test, Materials Science and Engineering A 532 (2009) 94-104.
[27] K.H. Jung, Y.T. Im, A Microstructure Evolution Model for Numerical Prediction of Austenite Grain Size Distribution, International Journal of Mechanical Sciences 52 (2010) 1136-1144.
[28] Kang S.H., Im Y.T., Three-Dimensional Finite Element Analysis of Quenching Process of Plain Carbon Steel with Phase Transformation, Metallurgical and Materials Transactions A 36 (2005) 2315-2325.
[29] S.H. Kang, Y.T. Im, Three-Dimensional Thermo-Elastic-Plastic Finite Element Modeling of Quenching Process of Plain-Carbon Steel in Couple with Phase Transformation, International Journal of Mechanical Sciences 49 (2007) 423-439.
[30] Y.T. Im, J.S. Cheon, S.H. Kang, Determination of Friction Condition by Geometrical Measurement of Backward Extruded Aluminum Alloy Specimen, Journal of Manufacturing Science and Engineering ASME 124 (2002) 409-415.
[31] Y.T. Im, S.H. Kang, J.S. Cheon, Finite Element Investigation of Friction Condition in a Backward Extrusion of Aluminum Alloy, Journal of Manufacturing Science and Engineering ASME 125 (2003) 378-383.
[32] S.H. Kang, J.H. Lee, J.S. Cheon, Y.T. Im, The Effect of Strain-Hardening on Frictional Behavior in Tip Test, International Journal of Mechanical Sciences 46 (2004) 855-869.
[33] P. Chauviere, K.H. Jung, D.K. Kim, H.C. Lee, S.H. Kang, Y.T. Im, Experimental Study of Miniaturized Tip Test, Journal of Mechanical Science and Technology 22 (2008) 924-930.
[34] Y.T. Im, S.H. Kang, J.S. Cheon, A Novel Technique of Friction and Material Property Measurement by Tip Test in Cold Forging, P.I. Mech. Eng. A-J. Eng. 220 (2006) 81-90.
[35] K.H. Jung, Y.T. Im, The Effect of Deformation Speed on Frictional Behavior by Tip Test, Journal of Tribology ASME Trans 132 (2010) 031801-1-6.
[36] K.H. Jung, H.C. Lee, J.S. Ajiboye, Y.T. Im, Characterization of Frictional Behavior in Cold Forging, Tribology Letters 37 (2010) 353-359.
[37] K.H. Jung. H.C. Lee, J.S. Ajiboye, S.H. Kang, Y.T. Im, The Effect of Surface Conditions on Friction by Tip Test, Journal of Tribology ASME Trans 132 (2010) 011601-1-7.
[38] K.H. Jung, D.K. Kim, S.H. Kang, Y.T. Im, Friction Measurement by the Tip Test for Cold Forging, Wear 286-287 (2012) 19-26.
[39] K.H. Jung, Y.T. Im, Determination of a Dimensionless Equation for Shear Friction Factor in Cold Forging, submitted to Wear, 2010.
[40] H.C. Lee, Y.G. Jin, Y.H. Lee, I.H. Son, D.L Lee, Y.T. Im, Process Design of High-Strength Bolt of Fully Pearlitic High-Carbon Steel, Journal of Materials Processing Technology 210 (2010) 1870-1875.
[41] H.C. Lee, Y.G. Jin, Y.H. Lee, S.K. Hwang, K.H. Jung, Y.T. Im, Wedge Tension Test of a High-Strength Bolt of Fully Pearlitic High-Carbon Steel, Journal of Materials Processing Technology 211 (2010) 1044-1050.

[42] J.H. Lee, I.H. Son, Y.T. Im, Finite Element Investigation of Equal Channel Angular Extrusion Process, Materials Transactions 45 (2004) 2165-2171.
[43] I.H. Son, Y.G. Jin, Y.T. Im, S.H. Chon, J.K. Park, Sensitivity of Friction Condition in Finite Element Investigations of Equal Channel Angular Extrusion, Materials Science and Engineering A 445 (2007) 676-685.
[44] Y.G. Jin, I.H. Son, S.H. Kang, Y.T. Im, Three-Dimensional Finite Element Analysis of Multi-Pass Equal-Channel Angular Extrusion of Aluminum AA1050 with Split Dies, Materials Science and Engineering A 503 (2009) 152-155.
[45] Y.G. Jin, I.H. Son, Y.T. Im, 3D Numerical and Experimental Study on Flow Characteristics of Multi-Pass ECAP with AA1050, International Journal of Modern Physics B 23 (2009) 1822-1828.
[46] J.S. Choi, S. Nawaz, S.K. Hwang, H.C. Lee, Y.T. Im, Forgeability of Ultra-Fine Grained Aluminum Alloy for Bolt Forming, International Journal of Mechanical Sciences 52 (2010) 1269-1276.
[47] Y.G. Jin, I.H. Son, Y.T. Im, Three-Dimensional Flow Characteristics of Aluminum Alloy in Multi-Pass Equal Channel Angular Pressing, Metals and Materials International 16 (2010) 413-420.
[48] Y.G. Jin, H.M. Baek, Y.T. Im, B.C. Jeon, Continuous ECAP Process Design for Manufacturing a Microstructure-Refined Bolt, Materials Science and Engineering A 530 (2012) 462-468.
[49] Y.G. Jin, H.M. Baek, S.K. Hwang, Y.T. Im, B.C. Jeon, Continuous High Strength Aluminum Bolt Manufacturing by the Spring-Loaded ECAP System, Journal of Materials Processing Technology 212 (2012) 848-855.
[50] S.K. Hwang, Y.G. Jin, H.M. Baek, D.K. Kim, Y.T. Im, A Continuous Hybrid Process for Manufacturing High-Strength Low Carbon Steel, Steel Research International Special Edition, Metal Forming (2011) 314-319.
[51] S.K. Hwang, Y.G. Jin, I.H. Son, K.H. Rhee, D.L. Lee, Y.T. Im, Flow Characteristics of Continuous Shear Drawing of High Carbon Steel, International Journal of Mechanical Sciences 53 (2011) 479-484.
[52] H.M. Baek, Y.G. Jin, S.K. Hwang, Y.T. Im, I.H. Son, D.L. Lee, Numerical Study on the Evolution of Surface Defects in Wire Drawing, Journal of Materials Processing Technology 212 (2012) 776-785.
[53] J.H. Kim, S.K. Hwang, Y.T. Im, I.H. Son, C.M. Bae, High-Strength Bolt-Forming of Fine-Grained Aluminum Alloy 6061 with a Continuous Hybrid Process, Materials Science and Engineering A 552 (2012)316-322.
[54] K.H. Jung, D.K. Kim, Y.T. Im, Y.S. Lee, Crystal Plasticity Finite Element Analysis of Texture Evolution during Rolling of FCC Polycrystalline Metal, submitted to International Journal of Mechanical Sciences 2012.
[55] K.H. Jung, D.K. Kim, Y.T. Im, Y.S. Lee, Prediction of the Effects of Hardening and Texture Heterogeneities based on the Crystal Plasticity Finite Element Method, submitted to International Journal of Plasticity 2012.
[56] H.W. Lee, Y.T. Im, Cellular Automata Modeling of Grain Coarsening and Refinement during the Dynamic Recrystallization of Pure Copper, Materials Transactions 51 (2010) 1614-1620.
[57] H.W. Lee, Y.T. Im, Numerical Modeling of Dynamic Recrystallization during Nonisothermal Hot Compression by Cellular Automata and Finite Element Analyses, International Journal of Mechanical Sciences 52 (2010) 1277-1289.
[58] D.K. Kim, K.H. Jung, H.W. Lee, Y.T. Im, Cellular Automata Simulation of Textural Evolution during Primary Static Recrystallization of IF Steel, Materials Science Forum 702-703 (2012) 615-618.